Assessment of 21 Days Lockdown Effect in Some States and Overall India: A Predictive Mathematical Study on COVID-19 Outbreak

Tridip Sardar [1a], Sk Shahid Nadim[b], Joydev Chattopadhyay[b]

[a]*Department of Mathematics, Dinabandhu Andrews College, Kolkata, India*
[b]*Agricultural and Ecological Research Unit, Indian Statistical Institute, Kolkata - 700 108, India*

Abstract

As of April, 6th, 2020, the total number of COVID-19 reported cases and deaths are 4778 and 136. This is an alarming situation as with a huge population within few days India will enter in stage-3 of COVID-19 transmission. In the absence of neither an effective treatment or vaccine and with an incomplete understanding of the epidemiological cycle, predictive mathematical models can help exploring of both COVID-19 transmission and control. In this present study, we consider a new mathematical model on COVID-19 transmission that incorporate lock-down effect and variability in transmission between symptomatic and asymptomatic populations with former being a fast spreader of the disease. Using daily COVID-19 notified cases from three states (Maharashtra, Delhi, and Telangana) and overall India, we assess the effect of current 21 days lock-down in terms of reduction cases and deaths. Lock-down effect is studied with different lock-down success rate. Our result suggest that 21 days lock-down will have no impact in Maharashtra and overall India. Furthermore, the presence of a higher percentage of COVID-19 super-spreaders will further deteriorate the situation in Maharashtra. However, for Tamil Nadu and Delhi there is some ray of hope as our prediction shows that lock-down will reduce a significant number of cases and deaths. in these two locations. Further extension of lock-down may place Delhi and Tamil Nadu in a comfort zone. Comparing estimated parameter samples for the mentioned four locations, we find a correlation between effect of lockdown and percentage of symptomatic infected in a region. Our result suggests that a higher percentage of symptomatic infected in a region leads to a large number of reduction in notified cases and deaths due to different lock-down scenario. Finally, we suggest a policy for the Indian Govt to control COVID-19 outbreak.

Keywords: COVID-19; Mathematical model; lock-down; Parameter estimation; Effective Reproduction Number.

[1]Corresponding author. Email: tridipiitk@gmail.com

1. Introduction

As of April 6, 2020, 13,46,004 cases and 74,654 deaths from 2019 novel coronavirus disease (COVID-19), caused by severe acute respiratory syndrome coronavirus 2 (SARS-CoV-2), were recorded worldwide [4]. Coronaviruses are enveloped non-segmented positive-sense RNA viruses that belongto the Coronaviridae family and the order Nidovirales, and are widely distributed among humans and other mammals [20]. The novel coronavirus, COVID-19 started in mainland China, with a geographical emphasis at Wuhan, the capital city of Hubei province [30] and has widely spread all over the world. Many of the initial cases were usually introduced to the wholesale Huanan seafood market, which also traded live animals. Clinical trials of hospitalized patients found that patients exhibit symptoms consistent with viral pneumonia at the onset of COVID-19, most commonly fever, cough, sore throat and fatigue [3]. Some patients reported changes in their ground-glass lungs; normal or lower than average white lymphocyte blood cell counts and platelet counts; hypoxemia; and deranged liver and kidney function. Most were said to be geographically related to the wholesale market of Huanan seafood [2]. Severe outbreaks occur in USA (3,67,004 cases), Italy (1,32,547 cases), Spain (1,36,675 cases), Germany (103,375 cases), France(98,010), China (81,708 cases) and so many countries and the disease continues to spread globally. This has been declared a pandemic by the World Health Organization. It is the third zoonotic human coronavirus that has arisen in the present century, after the 2002 severe acute respiratory syndrome coronavirus (SARS-CoV), which spread to 37 countries and the 2012 Middle East respiratory syndrome coronavirus (MERS-CoV), which spread to 27 countries.

The 2019 pandemic novel coronavirus was first confirmed in India on 30 January 2020, in the state of Kerala. A total of 4778 confirmed cases, 382 recoveries and 136 deaths in the country have been reported as of 6 April 2020 [5]. The Indian government has introduced social distance as a precaution to avoid the possibility of a large-scale population movement that can accelerate the spread of the disease. India government implemented a 14-hour voluntary public curfew on 22 March 2020. Furthermore, the Prime Minister of India also ordered a nationwide 21-day lockdown at midnight on 24 March to slow the spread of COVID-19, affecting India's entire 1.3 billion population. Despite no vaccine, social distancing has identified as the most commonly used prevention and control strategy [11]. The purpose of these initiatives is the restriction of social interaction in workplaces, schools, and other public spheres, except for essential public services such as fire, police, hospitals. No doubt the spread of this virus outbreak has seriously disrupted the life, economy and health of citizens. This is a great concern for everyone how long this scenario will last and when the disease will be controlled.

Mathematical modeling based on system of differential equations may provide a comprehensive mechanism for the dynamics of COVID-19 transmission. Several modeling studies have already been performed for the COVID-19 outbreak [27; 18; 24; 28; 16]. Based on data collected from December, 31^{st} 2019 till January, 28^{th} 2020, Wu et al. developed a susceptible exposed infectious recovered model (SEIR) to clarify the transmission dynamics and projected national and global spread of disease [31]. They also calculated around 2.68 is the basic reproductive number for COVID-19. Tang et al proposed a compartmental deterministic model that would combine the clinical development of the disease, the epidemiological status of the patient and the measures for intervention. Researchers found that the amount of control reproduction number may be as high as 6.47, and that methods of intervention including intensive touch tracing followed by quarantine and isolation would effectively minimize COVID cases [28]. For the basic reproductive number, Read et al. reported a value of 3.1 based on the data fitting of an SEIR model, using an assumption of Poisson-distributed daily time increments [19]. A report by Cambridge University has indicated that India's countrywide three-week lockdown would not be adequate to prevent a resurgence of the new coronavirus epidemic that could bounce back in months and cause thousands of infections [25]. They suggested that two or three lockdowns can extend the slowdown longer with five-day breaks in between or a single 49-day lockdown. Data-driven mathematical modeling plays a key role in disease prevention, planning for future outbreaks and determining the effectiveness of control. Several data-driven modeling experiments have been performed in various regions [28; 10]. Currently, there are very limited works that studied the impact of lock-down on COVID-19 transmission dynamics in India.

In the present manuscript, we proposed a new mathematical model for COVID-19 that incorporates the lock-down effect. We also considered variability in transmission between symptomatic and asymptomatic populations with former being a fast spreader of the disease. Using COVID-19 daily notified cases from three highly affected states (Maharashtra, Delhi, and Telangana) and from overall India, we estimated some key parameters of our model. In a large country like India with so much diverse population it is not at all feasible to lock-down (home quarantine) all susceptible population. A certain percentage of the population may be successfully home quarantined during the lock-down period. Thus, we assess the current 21 days (March, 25^{th} 2020 till April, 14^{th} 2020) lock-down scenario in India with different lock-down success rates. We studied the effect of different lock-down scenarios in terms of notified cases and deaths reduction for the four locations mentioned above for a certain time period. We estimated the basic reproduction number (R_0) for the mentioned four locations. Effective reproduction number is also estimated for different lock-down success rate using our model for these four regions.

2. Method

2.1. ***Model without lock-down***

Based on the development and epidemiological characteristics of COVID-19, a SEIR type model is more appropriate to study the dynamics of this current pandemic [14; 16; 17; 22]. The model we consider in this paper is an extension of a SEIR model with added asymptomatic $A(t)$ and hospitalized or notified $C(t)$ population (see Fig 1). As hospitalized or notified persons $C(t)$ are isolated and unable to contact susceptible individuals $S(t)$, we assume that disease transmission only occur in contact with asymptomatic ($A(t)$) and symptomatic $I(t)$ individuals (see Fig 1). We also assume variability in disease transmission in asymptomatic and symptomatic population with later being a fast spreader of infection with variability factor ρ. Recovery rate for asymptomatic, symptomatic and hospitalized or notified populations are assumed to be different with rates γ_1, γ_2, and γ_3, respectively. We considered disease related deaths (at a rate δ) only for hospitalized or notified population. Based on these assumptions, we develop the following compartmental model for COVID-19 outbreak:

$$\begin{aligned}
\frac{dS}{dt} &= \Pi_H - \frac{\beta_1 IS}{N} - \frac{\rho\beta_1 AS}{N} - \mu S \\
\frac{dE}{dt} &= \frac{\beta_1 IS}{N} + \frac{\rho\beta_1 AS}{N} - (\mu+\sigma)E, \\
\frac{dA}{dt} &= (1-\kappa)\sigma E - (\gamma_1+\tau_1+\mu)A, \\
\frac{dI}{dt} &= \kappa\sigma E - (\gamma_2+\tau_2+\mu)I, \\
\frac{dC}{dt} &= \tau_1 A + \tau_2 I - (\delta+\gamma_3+\mu)C, \\
\frac{dR}{dt} &= \gamma_1 A + \gamma_2 I + \gamma_3 C - \mu R,
\end{aligned} \tag{2.1}$$

where, $N(t)$ is the total human population at time t. A model (2.1) flow diagram is provided in Fig 1. Biological interpretations of model (2.1) parameters are provided in Table 1.

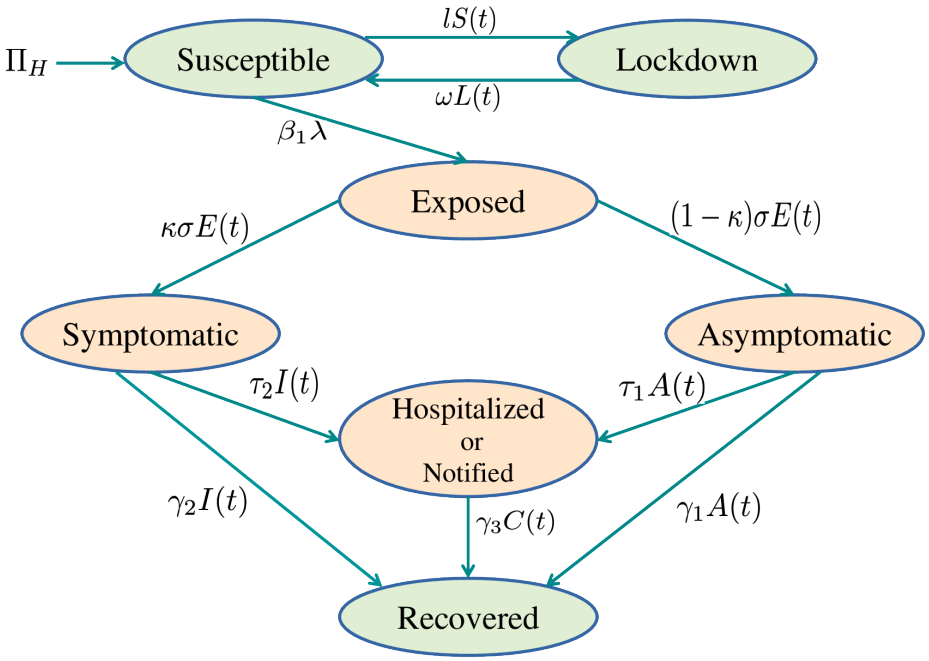

Figure 1: **Flow diagram of the model (2.1)**

Table 1: **Model (2.1) parameters with biological interpretations**

Parameters	Biological Meaning	Value/Ranges	Reference
$\Pi_H = \mu \times N(0)$	Recruitment rate of human population	-	-
$\frac{1}{\mu}$	Average life expectancy at birth	Varies over states	[1]
β_1	Transmission rate of Symptomatic infected	(0 - 200) day^{-1}	Estimated
ρ	Reduction in COVID-19 transmission for Asymptomatic infected	0 - 1	Estimated
$\frac{1}{\sigma}$	Incubation period for COVID-19	(1 - 14) $days$	Estimated
κ	Fraction of Exposed population that become Symptomatic infected	0 - 1	Estimated
γ_1	Recovery rate for Asymptomatic infected	(0 - 1) day^{-1}	Estimated
γ_2	Recovery rate for Symptomatic infected	(0 - 1) day^{-1}	Estimated
τ_1	Rate at which Asymptomatic infected become Hospitalized or Notified	(0 - 1) day^{-1}	Estimated
τ_2	Rate at which Symptomatic infected become Hospitalized or Notified	(0 - 1) day^{-1}	Estimated
δ	Death rate of Hospitalized or Notified population	Varies over states	[5]
γ_3	Recovery rate for Hospitalized or Notified Individuals	Varies over states	[5]

2.1.1. ***Model (2.1) with lock-down***

Lack of medicine or vaccine for COVID-19 infection only possible solution to containment may be lock-down of a large portion of the susceptible population. To model this scenario, we consider an added lock-down compartment $L(t)$ in the model (2.1). Lock-down population are fraction of the susceptible individuals that are home quarantined. Particularly, when the level of infection is high, people will be encouraged to

take the required steps to avoid contact with the infected individuals in order to protect themselves and their families, leading to a reduction in transmission levels. These rates of transmission also reflect a strong steps to control disease. We assume that a portion of the susceptible population become isolated due to lock-down at a success rate l. Since population which are isolated due to lock-down do not contact the infection therefore average effective contact rate of a single symptomatic and asymptomatic individual become $\frac{\beta_1}{(N-L)}$ and $\frac{\rho\beta_1}{(N-L)}$, respectively. We also assume that population in the lock-down compartment $L(t)$ again become susceptible after the lock-down period $(\frac{1}{\omega})$ is over. Based on these assumptions model (2.1) with lock-down become:

$$\begin{aligned}
\frac{dS}{dt} &= \Pi_H + \omega L - \frac{\beta_1 IS}{(N-L)} - \frac{\rho\beta_1 AS}{(N-L)} - \mu S - lS \\
\frac{dL}{dt} &= lS - (\mu+\omega)L, \\
\frac{dE}{dt} &= \frac{\beta_1 IS}{(N-L)} + \frac{\rho\beta_1 AS}{(N-L)} - (\mu+\sigma)E, \\
\frac{dA}{dt} &= (1-\kappa)\sigma E - (\gamma_1+\tau_1+\mu)A, \\
\frac{dI}{dt} &= \kappa\sigma E - (\gamma_2+\tau_2+\mu)I, \\
\frac{dC}{dt} &= \tau_1 A + \tau_2 I - (\delta+\gamma_3+\mu)C, \\
\frac{dR}{dt} &= \gamma_1 A + \gamma_2 I + \gamma_3 C - \mu R.
\end{aligned} \tag{2.2}$$

Here, l and $\frac{1}{\omega}$ are lock-down success rate and lock-down period respectively. Remaining parameters of the model (2.2) are given in Table 1.

2.1.2. ***Mathematical properties of the model*** (2.1)

We studied the positivity and boundedness of solution of the model (2.1) (See **Appendix A**). The system (2.1) demonstrates two equilibria, that is, the disease-free equlibrium and an unique endemic equilibrium (See **Appendix A**). The disease-free state is locally asymptotically stable whenever the corresponding basic reproduction number (R_0) is less than unity (See **Appendix A**). By using a nonlinear Lyapunov function, it is also seen that the disease-free equilibrium is globally asymptotically stable whenever $R_0 < 1$ (See **Appendix A**). In addition, the model (2.1) has an unique endemic equilibrium if R_0 exceeds unity. Furthermore, using the central manifold theory, the local stability of the endemic equilibrium is established whenever $R_0 > 1$ (See **Appendix A**).

2.1.3. ***Model calibration and COVID-19 data source***

Daily COVID-19 reported cases from Maharashtra, Delhi, Tamil Nadu and whole India for the time period March, 10^{th} 2020 till March, 29^{th} 2020 (for Maharashtra), March, 17^{th} 2020 till April, 2^{nd} 2020 (for Delhi), March, 18^{th} 2020 till April, 1^{st} 2020 (for Tamil Nadu), and March, 2^{nd} 2020 till March, 31^{st} 2020 (for India) are considered for our study. These three states are the most affected regions in India due to current COVID-19 pandemic [5]. Daily COVID-19 notified cases were collected from [5].

In Table 1, we listed the key parameters of the model (2.1) that are estimated from the data. We also estimated some unknown initial conditions of the model (2.1) from the data. MATLAB based nonlinear least square solver $fmincon$ is used to fit simulated and observed daily COVID-19 notified cases for these three states and the whole country during the mentioned time period. Delayed Rejection Adaptive Metropolis Hastings [12] algorithm is used to sample the 95% confidence region. An elaboration of this model fitting technique is provided in [23].

2.1.4. ***Prediction procedure***

In a large country like India with so much diverse population it is not at all feasible to lock-down (home quarantine) all susceptible population. A certain percentage of the population may be successfully home quarantined during the lock-down period. Thus, we assess the current 21 days (March, 25^{th} till April, 14^{th}) lock-down scenario in India with different success rate namely, 20%, 40%, 60%, and 80%, respectively. For example, a 20% lock-down success in Maharashtra means that 20% of the susceptible population in this state is successfully home quarantined during the lock-down time period.

To predict COVID-19 notified cases and as well deaths (daily and total) with different lock-down success rate, we undertake the following procedure.

- We run model (2.1) (without lock-down) using sample values of the estimated parameters and initial conditions (See **Appendix B**) till March, 25^{th} 2020. Using our simulation result, we predict the notified cases and deaths during this time duration.

- Using values of the state variables onset of the lock-down starting day on March, 25^{th} 2020 as initial condition, we simulate the model (2.2) (with lock-down) up to April, 14^{th}, 2020. Proceeding as earlier, we predict the notified cases and deaths during this time span.

- Again using values of the state variables onset of the lock-down ending day on April, 14^{th}, 2020 as initial condition, we run the model (2.1) (without lock-down) up to desired prediction period. Using result of this model run, we predict the notified cases and deaths during this time span.

- Finally, we ensemble all predicted cases and deaths during the whole time period.

2.1.5. ***Estimation of*** R_0***, and*** R_t

The Basic reproduction number (R_0) [29] for the model (2.1) is given as follows (see **Appendix A**):

$$R_0 = \frac{\beta_1 \kappa \sigma}{(\mu+\sigma)(\gamma_2+\tau_2+\mu)} + \frac{\rho\beta_1(1-\kappa)\sigma}{(\mu+\sigma)(\gamma_1+\tau_1+\mu)}. \tag{2.3}$$

The effective reproductive number (R_t) is defined as the expected number of secondary infection per infectious in a population made up of both susceptible and non-susceptible hosts [21]. If $R_t > 1$, the number of new cases will increase, for $R_t = 1$, the disease become endemic, and when $R_t < 1$ there will be a decline in the number of new cases.

Following [21], the expression of R_t is given as follows :

$$R_t = R_0 \times \hat{s}(t), \tag{2.4}$$

where, $\hat{s}(t)$ is the fraction of the host population that is susceptible at time t.

R_0 can easily be estimated by plugin the sample values of the unknown parameters in the expressions (2.3).

Following procedure is adapted to estimate R_t for different lock-down scenario:

- We first estimate R_0 using the estimated parameter values (see Table B5 in **Appendix B**) for the model (2.1).
- Proceeding as earlier, we run the models (2.1) and (2.2) at different time clusters (with and without lock-down). Using our simulation results, we estimate $\hat{s}(t)$ and R_t.

3. Results and discussion

Model (2.1) fitting to daily COVID-19 notified cases for Maharashtra, Delhi, Tamil Nadu and India is Depicted in Fig 2. Estimated values of the model (2.1) parameters and unknown initial conditions are provided in **Appendix B**, Table B1 and Table B2, respectively.

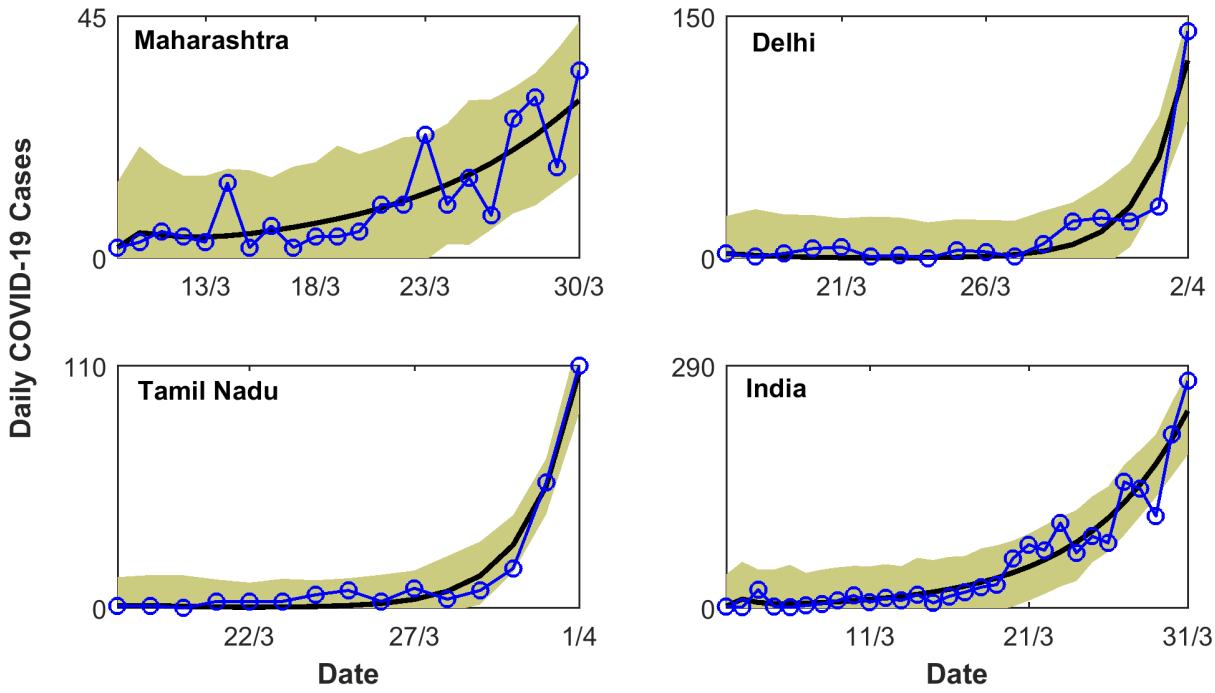

Figure 2: Model (2.1) fitting to daily notified COVID-19 cases in Maharashtra, Delhi, Tamil Nadu and India, respectively. Daily notified cases from these four locations are depicted in blue curve with circles and black curve is the solution of model (2.1). Yellow shaded region is the 95% confidence region.

In Maharashtra, estimate of symptomatic influx fraction (κ) suggesting low number (about 3%) of symptomatic infected in the population (See **Table B1** in **Appendix B**). However, higher value of the transmission rate (β_1), and low value of the transmission variability factor (ρ) indicates that existence of potential super-spreaders among symptomatic infected (see R_0 in equation (2.3) and **Table B1** in **Appendix B**). Low value of κ (see **Table B1** in **Appendix B**) indicates there may be a large number of undetected COVID-19 cases in the population of Maharashtra. However, low value of ρ indicates contribution of these asymptomatic infected towards new infection is very low (see expression of R_0 in equation (2.3) and **Table B1** in **Appendix B**). To further investigate on super-spreaders, we varies κ (from 0.1 to 0.5) in the expression of R_0. We found that around 60% - 92% increase in the current value of R_0 (see Table B5) if 10% to 50% new infection become symptomatic. This is an alarming situation as in coming days there may be a possibility of higher percentage of symptomatic infection and which leads to more and more super-spreaders in the population of Maharashtra.

We predicted notified cases as well deaths in Maharashtra for different lock-down situation (see **Methods section**) using our models with and without lock-down (see equations (2.1) and (2.2)) starting from March, 9^{th} 2020 till May, 7^{th} 2020 (60 days).

Predicted total notified cases and deaths under different (no lock-down, 20%, 40%, 60% and 80%) lock-down scenario in Maharashtra during the mentioned period is provided in Table B3 and Table B4, respectively. Furthermore, predicted daily notified cases and deaths under different (20%, 40%, 60% and 80%) lock-down scenario in Maharashtra during the mentioned period is depicted in Fig 3 and Fig 4, respectively. Our predictive study suggest that only 0.1% notified case reduction and $(0.3\% - 0.5\%)$ death reduction are possible under different lock-down circumstances in Maharashtra (see Table B3 and Table B4). Thus, 21 days lock-down will not improve current COVID-19 situation in Maharashtra.

For further investigate the lock-down effect in Maharashtra, we estimate the effective reproduction number (R_t) (see **Methods section**) for the period March, 9^{th} 2020 till May, 7^{th} 2020 under different lock-down scenario (no lock-down, 20%, 40%, 60% and 80%). Dynamics of R_t under different lock-down situation is depicted in Fig 5. Our result on R_t suggest that there may be a decrease in new cases during the lock-down period in Maharashtra (see Fig 5). However, after the lock-down is over on April, 15^{th} 2020 a sharp increase in R_t indicates that influx of new notified cases will rise again (see Fig 5). This result further support our claim that **lock-down in Maharashtra will not help its current COVID-19 situation**.

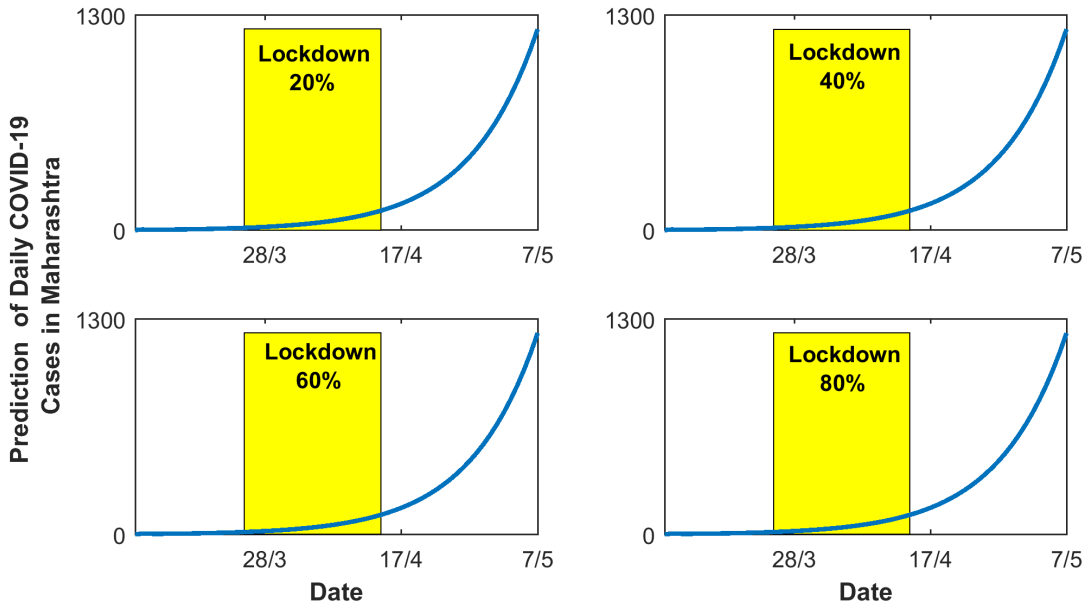

Figure 3: Model prediction of daily COVID-19 notified cases for the period 09/03/2020 till 07/05/2020 in Maharashtra with different lock-down scenario. Yellow bar is the current 21 days lock-down period (25/03/2020 till 14/04/2020) in Maharashtra. Lock-down scenarios are implemented with success rate 20%, 40%, 60% and 80% respectively. A lock-down success 20% in Maharashtra means that current implemented lock-down will successfully home-quarantine 20% of the total susceptible population.

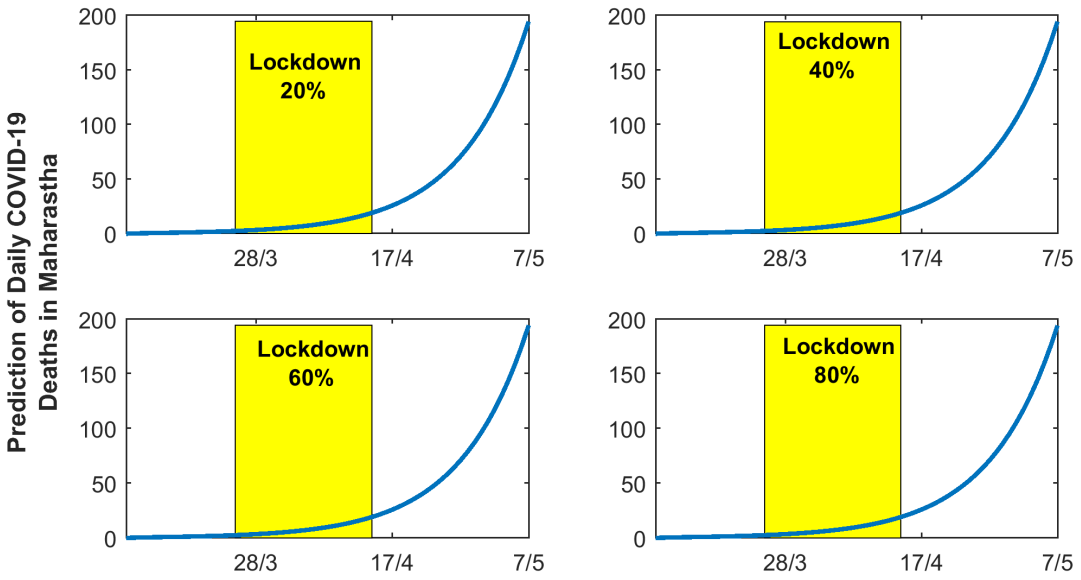

Figure 4: Model prediction of daily COVID-19 notified deaths for the period 09/03/2020 till 07/05/2020 in Maharashtra with different lock-down scenario. Yellow bar is the current 21 days lock-down period (25/03/2020 till 14/04/2020) in Maharashtra. Lock-down scenarios are implemented with success rate 20%, 40%, 60% and 80% respectively. A lock-down success 20% in Maharashtra means that current implemented lock-down will successfully home-quarantine 20% of the total susceptible population.

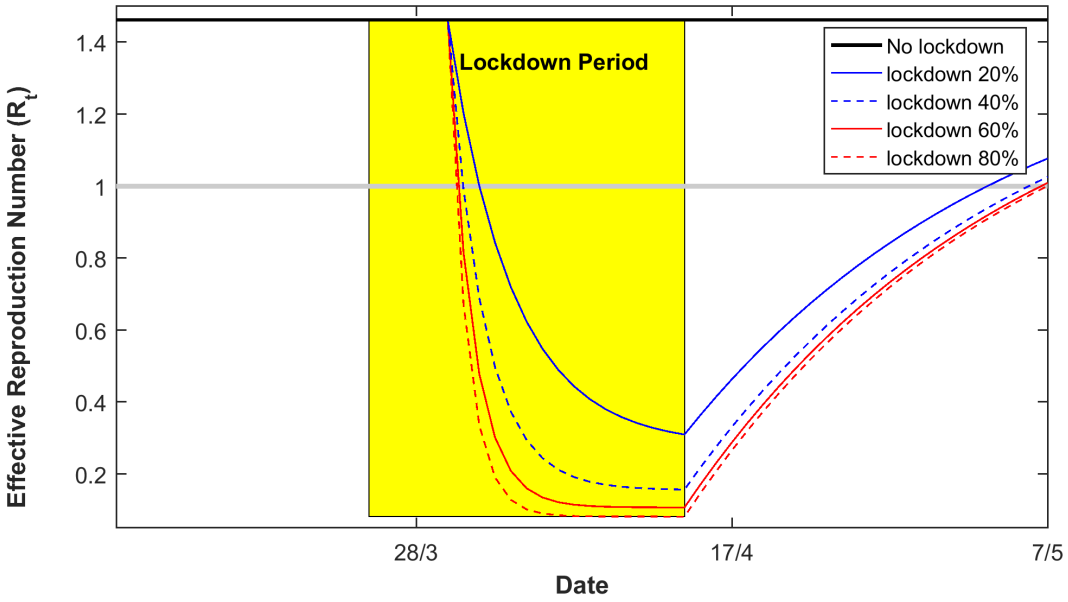

Figure 5: Effective reproduction number for the period 09/03/2020 till 07/05/2020 in Maharashtra with different lock-down scenario. Yellow interval is current 21 days lock-down period (25/03/2020 till 14/04/2020) in Maharashtra. Lock-down scenarios are implemented with success rate 0%, 20%, 40%, 60% and 80% respectively. Here, 0% lock-down success means no lock-down, and 20% represent current implemented lock-down will successfully home-quarantine 20% of the susceptible population in Maharashtra and similarly for other scenarios.

In Delhi, estimate of ρ (see **Table B1** in **Appendix B**) indicates as like Maharashtra here also contribution of asymptomatic infected in COVID-19 new infection is low. Higher value of κ (see **Table B1** in **Appendix B**) indicate that a higher percentage of symptomatic infected in Delhi. However, as estimate of disease transmission rate (β_1) is moderate (see **Table B1** in **Appendix B**) therefore there may be lower percentage of super-spreaders in Delhi. Estimate of R_0 in Delhi is provided in Table B5. Higher value **4.62 (3.70 - 5.40)** of R_0 (see Table B5) in Delhi may be due to presence of high percentage symptomatic infected in the population (see **Table B1** in **Appendix B**).

Notified cases as well as deaths in Delhi are predicted for different lock-down situations mentioned earlier (see **Method section**) staring from March, 17^{th} 2020 till May, 15^{th} 2020 (60 days). Predicted total notified cases and deaths under different (no lock-down, 20%, 40%, 60% and 80%) lock-down scenario in Delhi for the mentioned period is provided in Table B3 and Table B4, respectively. Daily predicted cases and deaths during the mentioned period in Delhi under different lock-down scenario is depicted in Fig 6 and Fig 7, respectively. Prediction of cases and deaths in Delhi (see Table B3 and Table B4) suggest that **(30% - 33%)** case reduction and **(39% - 52%)** death reduction are possible under different lock-down scenario. Thus, 21 days lock-down in Delhi will be effective

and should be extended for few weeks to further case and death reduction.

To further investigate the lock-down effect in Delhi, we estimate R_t (see **Method section**) for the period March, 17^{th} 2020 till May, 15^{th} 2020 under different lock-down scenario. Time-series of R_t for Delhi under different lock-down scenario is depicted in Fig 8. Estimate of R_t shows that it fall rapidly during the lock-down period (25/03/2020 till 14/04/2020) and shows some increment after lock-down is over (see Fig 8). However, R_t become saturated and remain below unity after the lock-down period is over (see Fig 8). This indicates that the number of new notified cases will decrease after the lock-down period (25/03/2020 till 14/04/2020) is over in Delhi. This result further support our claim that **21 days lock-down will be effective in Delhi and should be extended further for more cases and deaths reduction.**

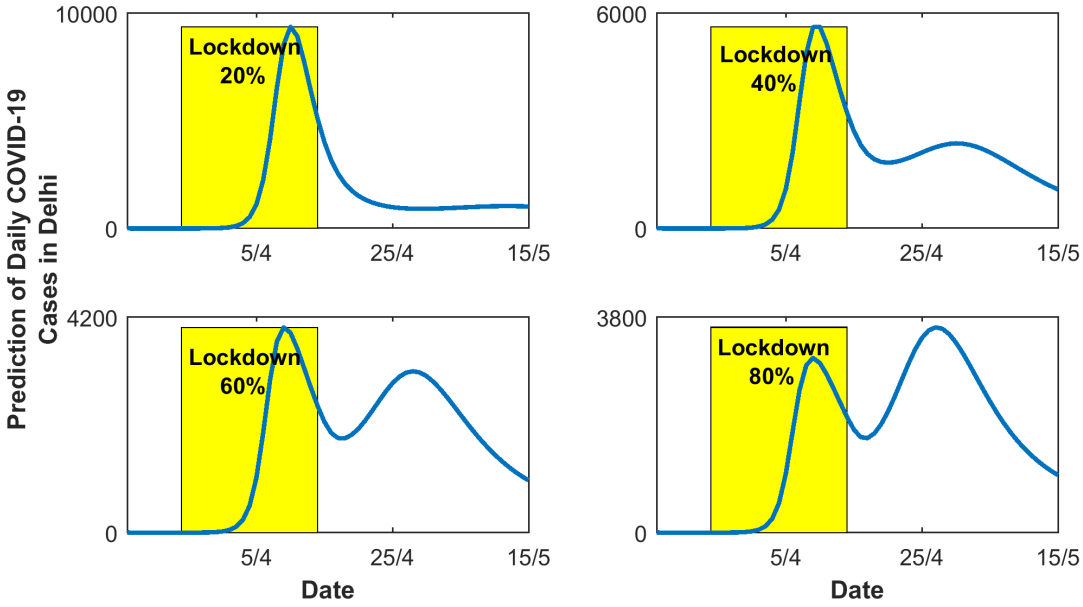

Figure 6: Model prediction of Daily COVID-19 notified cases for the period 17/03/2020 till 15/05/2020 in Delhi with different lock-down scenario. Yellow interval is current 21 days lock-down period (25/03/2020 till 14/04/2020) in Delhi. Lock-down scenarios are implemented with success rate 20%, 40%, 60% and 80% respectively. A lock-down success 20% in Delhi means that current implemented lock-down will successfully home-quarantine 20% of the total susceptible population.

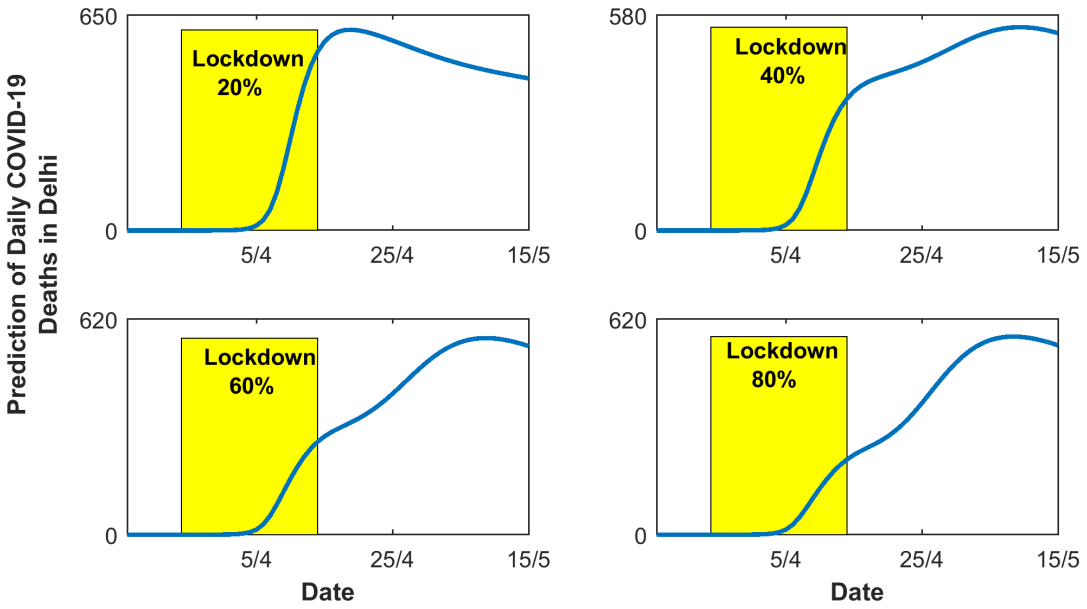

Figure 7: Model prediction of Daily COVID-19 deaths for the period 17/03/2020 till 15/05/2020 in Delhi with different lock-down scenario. Yellow interval is current 21 days lock-down period (25/03/2020 till 14/04/2020) in Delhi. Lock-down scenarios are implemented with success rate 20%, 40%, 60% and 80% respectively. A lock-down success 20% in Delhi means that current implemented lock-down will successfully home-quarantine 20% of the total susceptible population.

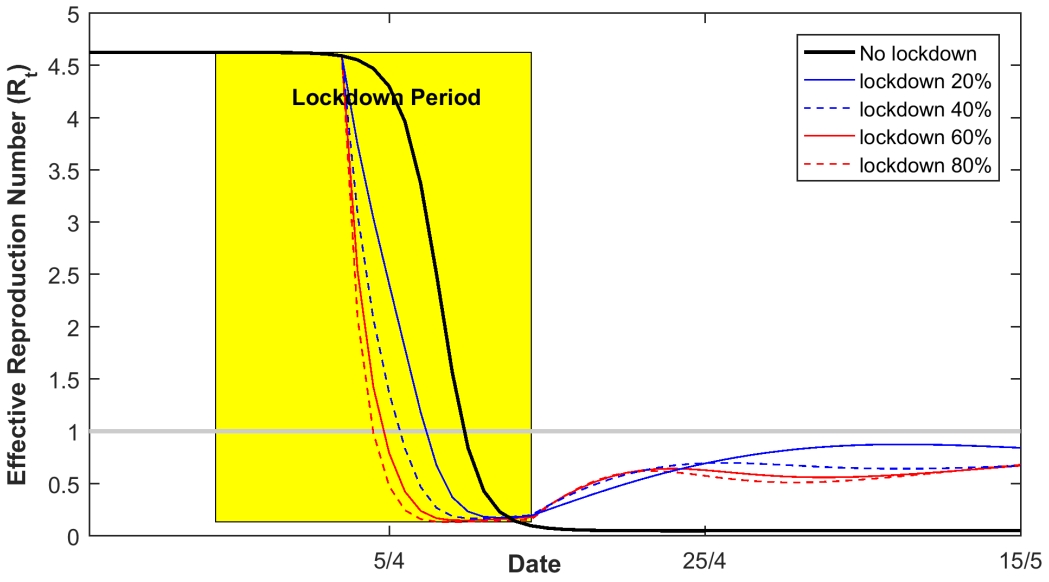

Figure 8: Effective reproduction number for the period 17/03/2020 till 15/05/2020 in Delhi with different lock-down scenario. Yellow interval is the current 21 days lock-down period (25/03/2020 till 14/04/2020) in Delhi. Lock-down scenarios are implemented with success rate 0%, 20%, 40%, 60% and 80% respectively. Here, 0% lock-down success means no lock-down, and 20% represent current implemented lock-down will successfully home-quarantine 20% of the susceptible population in Delhi and similarly for other scenarios.

In Tamil Nadu, estimate of ρ (see **Table B1** in **Appendix B**) indicate that here asymptomatic infected population contribute higher in producing new COVID-19 cases in compare to Maharashtra and Delhi (see expression of R_0 in equation (2.3) and **Table B1** in **Appendix B**). As percentage of symptomatic infected (see **Table B1** in **Appendix B**) in the population is also very high in Tamil Nadu, therefore, the estimate of R_0, **8.44 (5.20 - 13.23)**, for Tamil Nadu found out to be much higher than Maharashtra, Delhi and overall India (see Table B5).

Notified cases and deaths in Tamil Nadu are predicted for different lock-down scenario as mentioned earlier (see **Method section**) starting from March, 18^{th} 2020 till May, 16^{th} 2020 (60 days). Predicted total notified cases and deaths under different (no lock-down, 20%, 40%, 60% and 80%) lock-down situation in Tamil Nadu for the mentioned time duration are provided in Table B3 and Table B4, respectively. Predicted daily notified cases and deaths for the mentioned time interval under different lock-down circumstances are depicted in Fig 9 and Fig 10, respectively. Predicted cases and deaths in Tamil Nadu (see Table B3 and Table B4) suggest that (21% - 29%) notified case reduction and (32% - 48%) notified death reduction are possible under different lock-down scenario. Therefore, our prediction result suggest that 21 days lock-down in Tamil-Nadu will be effective if it

is extended further for few more weeks.

For further investigation in lock-down situation in Tamil Nadu, we estimate R_t (see **Method section**) for the time period March, 18^{th} 2020 till May, 16^{th} 2020 under different lock-down scenario. Dynamics of R_t for Tamil Nadu under different lock-down scenario for the mentioned time duration is depicted in Fig 11. R_t falls rapidly during the lock-down period (25/03/2020 till 14/04/2020) and after that it become almost stagnant (below unity). This shows that number of new cases in Tamil Nadu will fall after lock-down period is over. Therefore it is **high time to implement few weeks lock-down again in Tamil Nadu after the current lock-down period is over.**

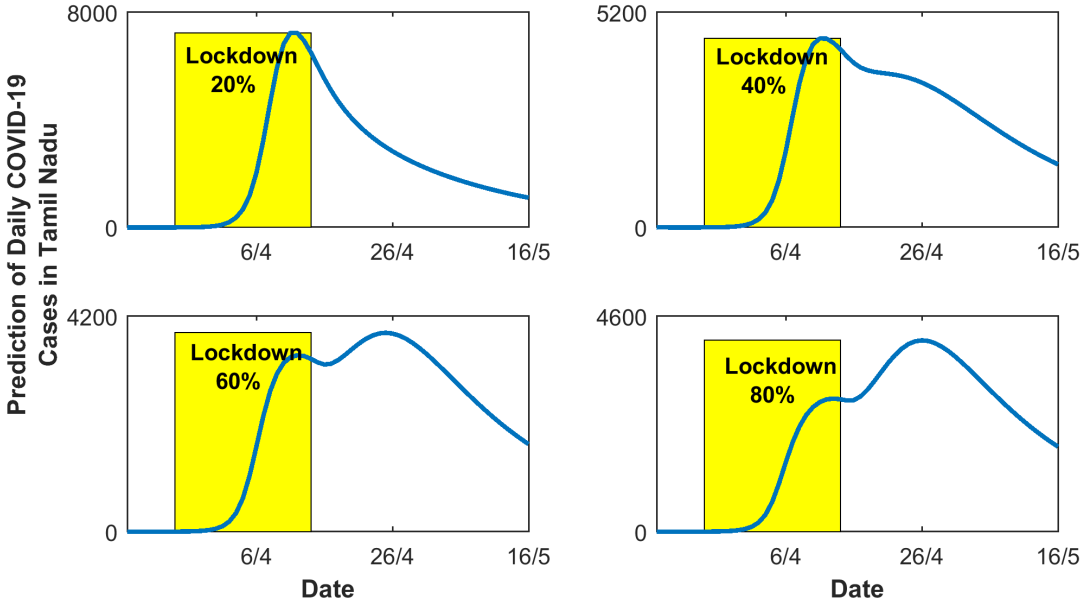

Figure 9: Model prediction of Daily COVID-19 cases for the period 18/03/2020 till 16/05/2020 in Tamil Nadu with different lock-down scenario. Yellow interval is the current 21 days lock-down period (25/03/2020 till 14/04/2020) in Tamil Nadu. Lock-down scenarios are implemented with success rate 20%, 40%, 60% and 80% respectively. A lock-down success 20% in Tamil Nadu means that current implemented lock-down will successfully home-quarantine 20% of the total susceptible population.

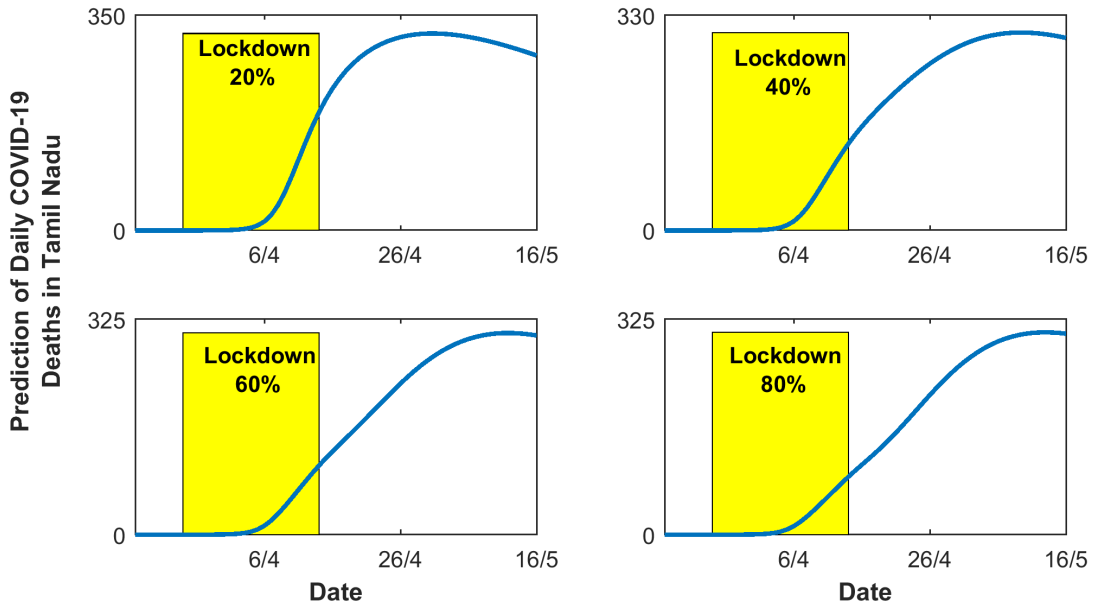

Figure 10: Model prediction of Daily COVID-19 deaths for the period 18/03/2020 till 16/05/2020 in Tamil Nadu with different lock-down scenario. Yellow interval is the current 21 days lock-down period (25/03/2020 till 14/04/2020) in Tamil Nadu. Lock-down scenarios are implemented with success rate 20%, 40%, 60% and 80% respectively. A lock-down success 20% in Tamil Nadu means that current implemented lock-down will successfully home-quarantine 20% of the total susceptible population.

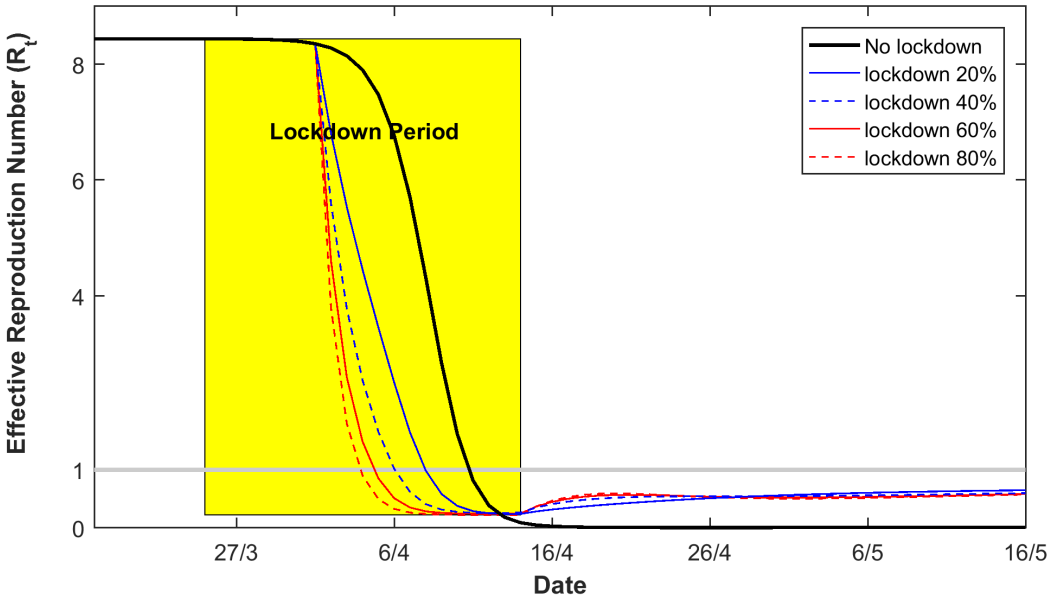

Figure 11: Effective reproduction number for the period 18/03/2020 till 16/05/2020 in Tamil Nadu with different lock-down scenarios. Yellow interval is the current 21 days lock-down period (25/03/2020 till 14/04/2020) in Tamil Nadu. Lock-down scenarios are implemented with success rate 0%, 20%, 40%, 60% and 80% respectively. Here, 0% lock-down success means no lock-down, and 20% represent current implemented lock-down will successfully home-quarantine 20% of the susceptible population in Tamil Nadu and similarly for other scenarios.

Overall in India, estimate of κ (see **Table B1** in **Appendix B**) suggest that there is large number of undetected cases in the population. Furthermore, the estimate of ρ (see R_0 in equation (2.3) and **Table B1** in **Appendix B**) suggest that these large undetected cases contribute a notable amount in producing new COVID-19 cases. Estimate of β_1 (see **Table B1** in **Appendix B**) in overall India found out in resemblance with its values for Delhi and Tamil Nadu. Estimate of the basic reproduction number (R_0) for overall India is provided in Table B5.

Notified cases as well as deaths in India are predicted for different lock down situation (see **Method section**) mentioned earlier starting from March, 2^{nd} 2020 till May, 7^{th} 2020 (67 days). Predicted total notified cases and deaths under different lock-down scenario (no-lock-down, 20%, 40%, 60%, and 80%) in India for the mentioned time span are provided in Table B3 and TableB4, respectively. Predicted daily notified cases and deaths in India for the mentioned time duration under different lock-down scenario are depicted in Fig 12 and Fig 13, respectively. Predicted cases and deaths in India (see Table B3 and TableB4) suggest that (0.2% - 0.6%) notified case reduction and (0.2% - 0.5%) notified death reduction are possible under different lock-down circumstances. Thus, 21 days lock-down will not improve current COVID-19 situation in overall India.

To further investigate in this direction, we estimate R_t (see **Method section**) for the time period March, 2^{nd} 2020 till May, 7^{th} 2020 under different lock-down scenario. Dynamics of R_t under different lock-down scenario for the mentioned time duration is depicted in Fig 14. Dynamics of R_t over the mentioned time duration suggest that there may be decrease in new cases during the lock-down period in India. However, sharp increase in R_t after the lock-down period indicates that daily notified cases will rise again (see Fig 14). This result further support our claim that **21 days lock-down will not improve current COVID-19 situation in overall India**. Our claim in resemblance with a recent COVID-19 study on overall India [25].

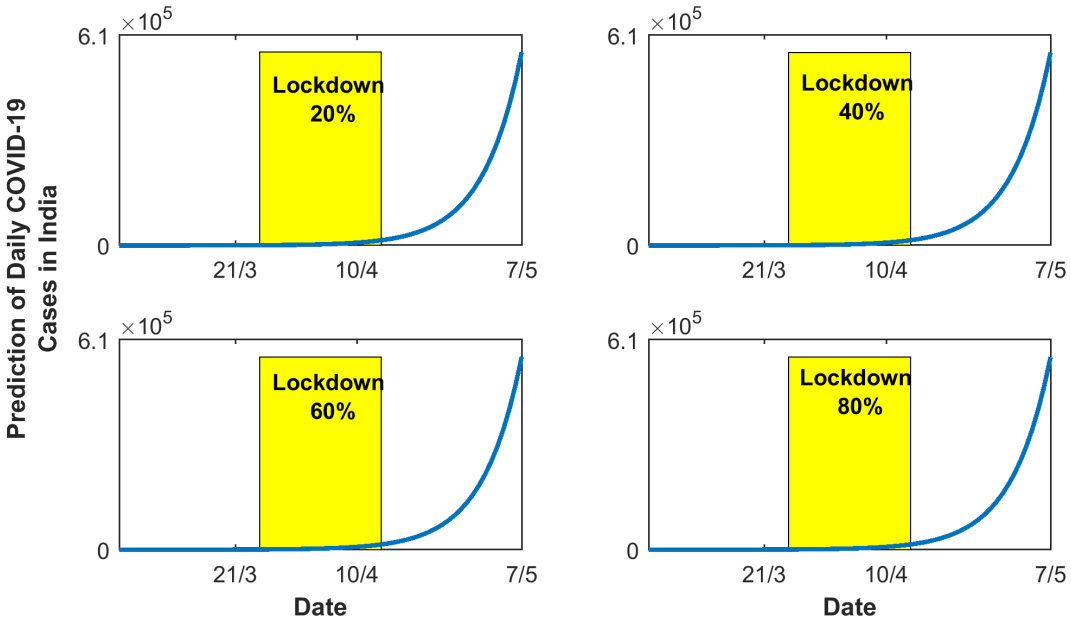

Figure 12: Model prediction of Daily COVID-19 cases for the period 02/03/2020 till 07/05/2020 in India with different lock-down scenario. Yellow interval is the current 21 days lock-down period (25/03/2020 till 14/04/2020) in India. Lock-down scenarios are implemented with success rate 20%, 40%, 60% and 80% respectively. A lock-down success 20% in India means that current implemented lock-down will successfully home-quarantine 20% of the total susceptible population.

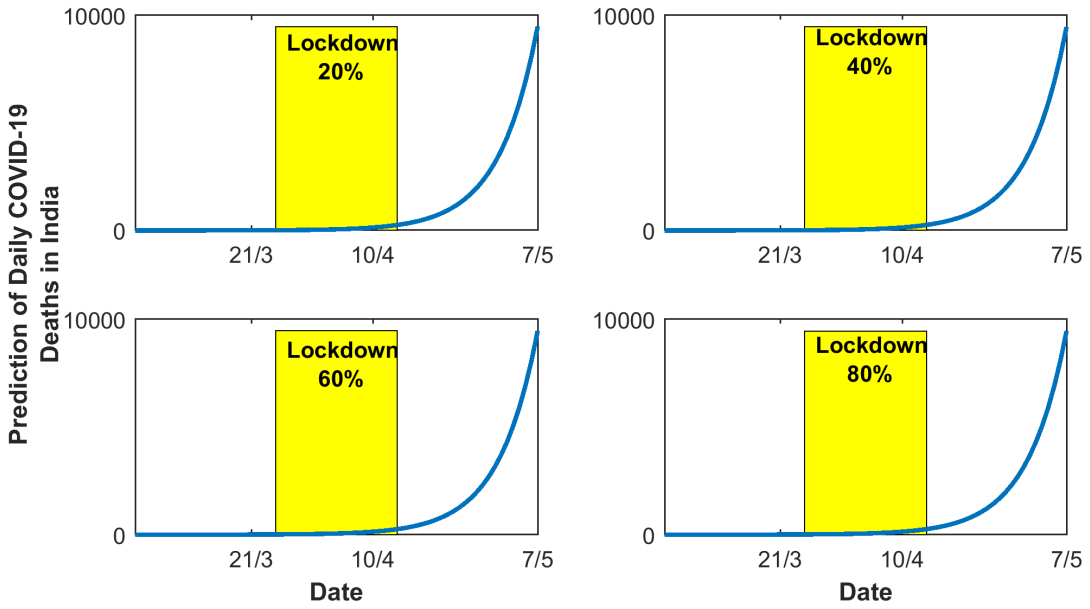

Figure 13: Model prediction of Daily COVID-19 deaths for the period 02/03/2020 till 07/05/2020 in India with different lock-down scenario. Yellow interval is the current 21 days lock-down period (25/03/2020 till 14/04/2020) in India. Lock-down scenarios are implemented with success rate 20%, 40%, 60% and 80% respectively. A lock-down success 20% in India means that current implemented lock-down will successfully home-quarantine 20% of the total susceptible population.

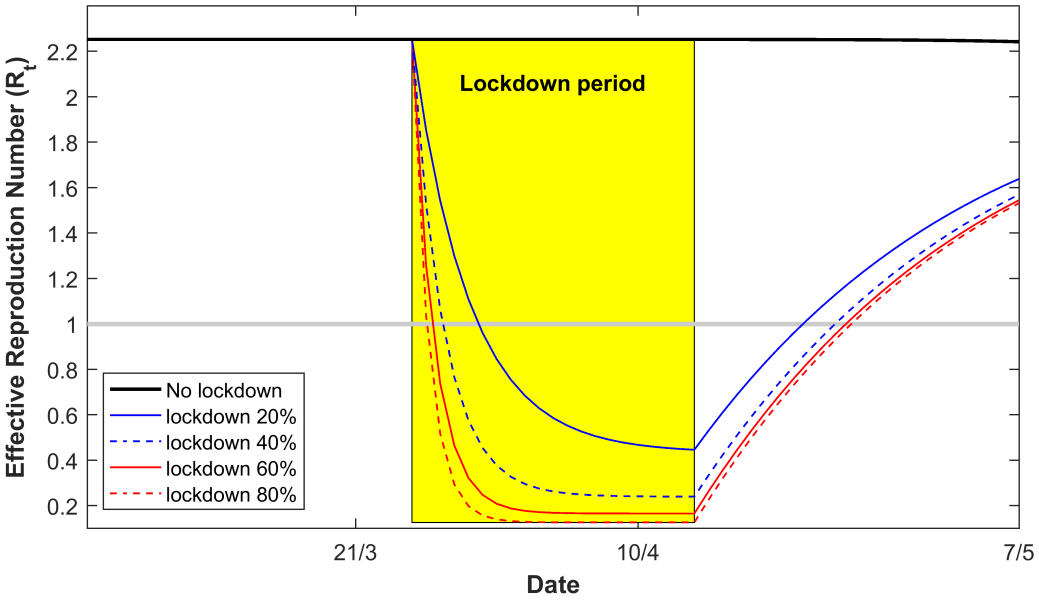

Figure 14: Effective reproduction number for the period 02/03/2020 till 07/05/2020 in India with different lock-down scenarios. Yellow interval is the current 21 days lock-down period (25/03/2020 till 14/04/2020) in India. Lock-down scenarios are implemented with success rate 0%, 20%, 40%, 60% and 80% respectively. Here, 0% lock-down success means no lock-down, and 20% represent current implemented lock-down will successfully home-quarantine 20% of the susceptible population in India and similarly for other scenarios.

4. Conclusion

Up to April, 6^{th}, 2020, total number of reported COVID-19 cases and deaths in India are **4778** and **136**, respectively [5]. This tally rises with few hundred new notified cases every day reported from different locations in India [5]. This is an alarming situation as with a huge population within few days India will enter in stage-3 of COVID-19 transmission. In the absence of neither a effective treatment or vaccine and with an incomplete understanding of epidemiological cycle, predictive mathematical models can help strengthen our understanding of both COVID-19 transmission and control [22].

In this present study, we consider a new mathematical model on COVID-19 transmission that incorporates the lock-down effect. In our model, we also considered transmission variability between symptomatic and asymptomatic population with former being a fast spreader of the disease. Using daily notified cases from three states (Maharashtra, Delhi, and Tamil Nadu) and form whole India, we studied the effect of 21 days lock-down (25/03/2020 till 14/04/2020) on notified cases and deaths reduction in those regions. Our result suggest that Lock-down will have no effect in Maharashtra and overall India. Furthermore, presence of higher percentage of COVID-19 super-spreaders will further

deteriorate the situation in Maharashtra. However, for Delhi and Tamil Nadu there is some ray of hope as our prediction shows that lock-down will reduce significant number of notified cases and deaths in these two locations. Further extension of lock-down may place Delhi and Tamil Nadu in a comfort zone. To find the answer of the question **why lock-down have some effect in Delhi and Tamil Nadu but no effect on overall India and Maharashtra?** We closely look at the parameters sample table for these four locations (see Table B1) and found that in Tamil Nadu and Delhi there is a large percentage of symptomatic infected exists in the population. Whereas, in Maharashtra and overall India percentage of symptomatic infected population is very low (see Table B1). Thus, there may be a possibility that larger proportion of symptomatic infected in a population can help epidemic curve to reach its peak quickly. To further investigate our claim, we simulate new notified cases for these four locations with mentioned prediction period without any lock-down (see Fig 15). It can be easily seen from Fig 15, that in Delhi and Tamil-Nadu notified new cases reaches the epidemic peak and whereas for Maharashtra and overall India notified cases slowly increases and still increasing during the mentioned time duration. As new notified cases in Delhi and Tamil Nadu grow faster therefore, 21 days lock-down has some significant impact in reducing cases and deaths in these two locations. Thus, 21 days lock-down may be effective in reducing significant amount of cases and deaths in those location in India where percentage of symptomatic infected population is higher. Finally, we provide a suggestion for the Indian Govt. and Policy makers to do the following steps:

1. **An extensive survey to find the percentage of symptomatic infected in different states and regions.**
2. **Focus implementing extensive lock-down in those locations only where the percentage of symptomatic infected is very high.**
3. **Provide relaxation in lock-down in other locations for some time. This will increase the percentage of symptomatic infection.**
4. **Repeat step-2, when a region has a sufficient percentage of the symptomatic infected.**

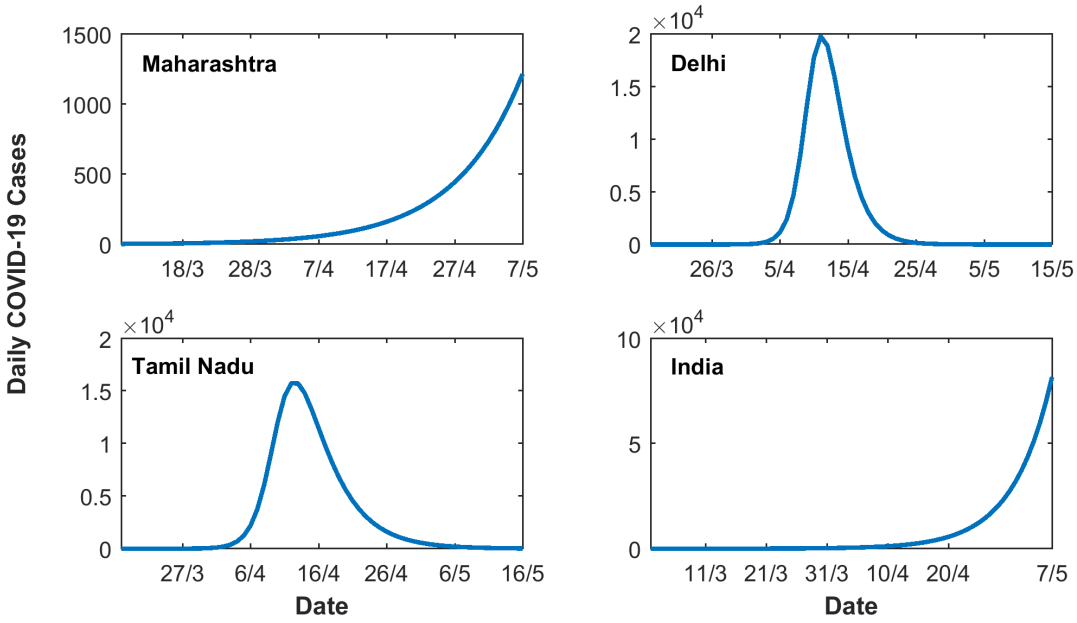

Figure 15: Model predicted Daily COVID-19 notified cases for Maharashtra, Delhi, Tamil Nadu and India.

Conflict of interests

The authors declare that they have no conflicts of interest.

Acknowledgments

Dr. Tridip Sardar acknowledges the Science & Engineering Research Board (SERB) major project grant (File No: EEQ/2019/000008 dt. 4/11/2019), Government of India.

Sk Shahid Nadim receives funding as senior research fellowship from Council of Scientific & Industrial Research (Grant No: 09/093(0172)/2016/EMR-I), Government of India, New Delhi.

The Funder had no role in study design, data collection and analysis, decision to publish, or preparation of the manuscript.

References

[1] Life expectancy at birth. http://statisticstimes.com/demographics/population-of-indian-states.php, 2019. Retrieved : 2020-04-05.

[2] Wuhan wet market closes amid pneumonia outbreak. https://www.chinadaily.com.cn/a/202001/01/WS5e0c6a49a310cf3e35581e30.html, 2019. Retrieved : 2020-03-04.

[3] Centers for disease control and prevention: 2019 novel coronavirus. https://www.cdc.gov/coronavirus/2019-ncov, 2020. Retrieved : 2020-03-10.

[4] Coronavirus covid-19 global cases by the center for systems science and engineering. https://gisanddata.maps.arcgis.com/apps/opsdashboard/index.html#/bda7594740fd40299423467b48e9ecf6, 2020. Retrieved : 2020-04-02.

[5] India covid-19 tracker. https://www.covid19india.org/, 2020. Retrieved : 2020-04-03.

[6] Ministry of health and family welfare government of india. https://www.mohfw.gov.in/, 2020. Retrieved : 2020-04-03.

[7] Roy M Anderson, B Anderson, and Robert M May. *Infectious diseases of humans: dynamics and control*. Oxford university press, 1992.

[8] Roy M Anderson and Robert M May. Population biology of infectious diseases: Part i. *Nature*, 280(5721):361–367, 1979.

[9] Carlos Castillo-Chavez and Baojun Song. Dynamical models of tuberculosis and their applications. *Mathematical Biosciences & Engineering*, 1(2):361, 2004.

[10] Tianmu Chen, Jia Rui, Qiupeng Wang, Zeyu Zhao, Jing-An Cui, and Ling Yin. A mathematical model for simulating the transmission of wuhan novel coronavirus. *bioRxiv*, 2020.

[11] Neil Ferguson, Daniel Laydon, Gemma Nedjati Gilani, Natsuko Imai, Kylie Ainslie, Marc Baguelin, Sangeeta Bhatia, Adhiratha Boonyasiri, ZULMA Cucunuba Perez, Gina Cuomo-Dannenburg, et al. Report 9: Impact of non-pharmaceutical interventions (npis) to reduce covid19 mortality and healthcare demand. 2020.

[12] Heikki Haario, Marko Laine, Antonietta Mira, and Eero Saksman. Dram: efficient adaptive mcmc. *Statistics and computing*, 16(4):339–354, 2006.

[13] Herbert W Hethcote. The mathematics of infectious diseases. *SIAM review*, 42(4):599–653, 2000.

[14] Adam J Kucharski, Timothy W Russell, Charlie Diamond, Yang Liu, John Edmunds, Sebastian Funk, Rosalind M Eggo, Fiona Sun, Mark Jit, James D Munday,

et al. Early dynamics of transmission and control of covid-19: a mathematical modelling study. *The Lancet Infectious Diseases*, 2020.

[15] Joseph P LaSalle. *The stability of dynamical systems*, volume 25. Siam, 1976.

[16] Sk Shahid Nadim, Indrajit Ghosh, and Joydev Chattopadhyay. Short-term predictions and prevention strategies for covid-2019: A model based study. *arXiv preprint arXiv:2003.08150*, 2020.

[17] Liangrong Peng, Wuyue Yang, Dongyan Zhang, Changjing Zhuge, and Liu Hong. Epidemic analysis of covid-19 in china by dynamical modeling. *arXiv preprint arXiv:2002.06563*, 2020.

[18] Billy J Quilty, Sam Clifford, et al. Effectiveness of airport screening at detecting travellers infected with novel coronavirus (2019-ncov). *Eurosurveillance*, 25(5), 2020.

[19] Jonathan M Read, Jessica RE Bridgen, Derek AT Cummings, Antonia Ho, and Chris P Jewell. Novel coronavirus 2019-ncov: early estimation of epidemiological parameters and epidemic predictions. *MedRxiv*, 2020.

[20] Douglas D Richman, Richard J Whitley, and Frederick G Hayden. *Clinical virology*. John Wiley & Sons, 2016.

[21] Kenneth J Rothman, Sander Greenland, and Timothy L Lash. *Modern epidemiology*. Lippincott Williams & Wilkins, 2008.

[22] Tridip Sardar, Indrajit Ghosh, Xavier Rodó, and Joydev Chattopadhyay. A realistic two-strain model for mers-cov infection uncovers the high risk for epidemic propagation. *PLOS Neglected Tropical Diseases*, 14(2):e0008065, 2020.

[23] Tridip Sardar and Bapi Saha. Mathematical analysis of a power-law form time dependent vector-borne disease transmission model. *Mathematical biosciences*, 288:109–123, 2017.

[24] Mingwang Shen, Zhihang Peng, Yanni Xiao, and Lei Zhang. Modelling the epidemic trend of the 2019 novel coronavirus outbreak in china. *bioRxiv*, 2020.

[25] Rajesh Singh and R Adhikari. Age-structured impact of social distancing on the covid-19 epidemic in india. *arXiv preprint arXiv:2003.12055*, 2020.

[26] Hal L Smith and Paul Waltman. *The theory of the chemostat: dynamics of microbial competition*, volume 13. Cambridge university press, 1995.

[27] Biao Tang, Nicola Luigi Bragazzi, Qian Li, Sanyi Tang, Yanni Xiao, and Jianhong Wu. An updated estimation of the risk of transmission of the novel coronavirus (2019-ncov). *Infectious Disease Modelling*, 5:248–255, 2020.

[28] Biao Tang, Xia Wang, Qian Li, Nicola Luigi Bragazzi, Sanyi Tang, Yanni Xiao, and Jianhong Wu. Estimation of the transmission risk of the 2019-ncov and its implication for public health interventions. *Journal of Clinical Medicine*, 9(2):462, 2020.

[29] Pauline Van den Driessche and James Watmough. Reproduction numbers and sub-threshold endemic equilibria for compartmental models of disease transmission. *Mathematical biosciences*, 180(1-2):29–48, 2002.

[30] Chen Wang, Peter W Horby, Frederick G Hayden, and George F Gao. A novel coronavirus outbreak of global health concern. *The Lancet*, 395(10223):470–473, 2020.

[31] Joseph T Wu, Kathy Leung, and Gabriel M Leung. Nowcasting and forecasting the potential domestic and international spread of the 2019-ncov outbreak originating in wuhan, china: a modelling study. *The Lancet*, 395(10225):689–697, 2020.

[32] Xia Yang, Lansun Chen, and Jufang Chen. Permanence and positive periodic solution for the single-species nonautonomous delay diffusive models. *Computers & Mathematics with Applications*, 32(4):109–116, 1996.

Appendix A

4.1. Positivity and boundedness of the solution for the Model (2.1)

This subsection is provided to prove the positivity and boundedness of solutions of the system (2.1) with initial conditions $(S(0), E(0), A(0), I(0), C(0), R(0))^T \in \mathbb{R}^6_+$. We first state the following lemma.

Lemma 4.1. *Suppose* $\Omega \subset \mathbb{R}\times\mathbb{C}^n$ *is open,* $f_i \in C(\Omega, \mathbb{R}), i = 1, 2, 3, ..., n$. *If* $f_i|_{x_i(t)=0, X_t\in\mathbb{C}^n_{+0}} \geq 0$, $X_t = (x_{1t}, x_{2t}, ..., x_{1n})^T, i = 1, 2, 3, ..., n$, *then* $\mathbb{C}^n_{+0}\{\phi = (\phi_1, ..., \phi_n) : \phi \in \mathbb{C}([-\tau, 0], \mathbb{R}^n_{+0})\}$ *is the invariant domain of the following equations*

$$\frac{dx_i(t)}{dt} = f_i(t, X_t), t \geq \sigma, i = 1, 2, 3, ..., n.$$

where $\mathbb{R}^n_{+0} = \{(x_1, ...x_n) : x_i \geq 0, i = 1, ..., n\}$ *[32].*

Proposition 4.1. *The system (2.1) is invariant in* $\mathbb{R}^6_+$.

Proof. By re-writing the system (2.1) we have

$$\frac{dX}{dt} = B(X(t)), X(0) = X_0 \geq 0 \tag{A-1}$$

$B(X(t)) = (B_1(X), B_1(X), ..., B_6(X))^T$
We note that

$$\frac{dS}{dt}|_{S=0} = \Pi_H \geq 0, \frac{dE}{dt}|_{E=0} = \frac{\beta_1 S(I + \rho A)}{N} \geq 0, \frac{dA}{dt}|_{A=0} = (1-\kappa)\sigma E \geq 0,$$
$$\frac{dI}{dt}|_{I=0} = \kappa\sigma E \geq 0, \frac{dC}{dt}|_{C=0} = \tau_1 A + \tau_2 I \geq 0, \frac{dR}{dt}|_{R=0} = \gamma_1 A + \gamma_2 I + \gamma_3 C \geq 0.$$

Then it follows from the Lemma 4.1 that $\mathbb{R}^6_+$ is an invariant set. □

Lemma 4.2. *The system (2.1) is bounded in the region*
$\Omega = \{(S, E, A, I, C, R \in \mathbb{R}^6_+ | S + E + A + I + C + R \leq \frac{\Pi_H}{\mu}\}$

Proof. We observed from the system that

$$\frac{dN}{dt} = \Pi_H - \mu N - \delta C \leq \Pi_H - \mu N$$
$$\Longrightarrow \lim_{t\to\infty} supN(t) \leq \frac{\Pi_H}{\mu}$$

Hence the system (2.1) is bounded. □

4.2. Local stability of disease-free equilibrium (DFE)

The DFE of the model (2.1) is given by

$$\begin{aligned}\varepsilon_0 &= (S^0, E^0, A^0, I^0, C^0, R^0)\\ &= \left(\frac{\Pi_H}{\mu}, 0, 0, 0, 0, 0, 0\right)\end{aligned}$$

The local stability of ε_0 can be established on the system (2.1) by using the next generation operator method. Using the notation in [29], the matrices F for the new infection and V for the transition terms are given, respectively, by

$$F = \begin{bmatrix} 0 & \rho\beta_1 & \beta_1 & 0 \\ 0 & 0 & 0 & 0 \\ 0 & 0 & 0 & 0 \\ 0 & 0 & 0 & 0 \end{bmatrix},$$

$$V = \begin{bmatrix} \mu+\sigma & 0 & 0 & 0 \\ -(1-\kappa)\sigma & \gamma_1+\tau_1+\mu & 0 & 0 \\ -\kappa\sigma & 0 & \gamma_2+\tau_2+\mu & 0 \\ 0 & -\tau_1 & -\tau_2 & \delta+\gamma_3+\mu \end{bmatrix}.$$

It follows that the basic reproduction number [13], denoted by $R_0 = \rho(FV^{-1})$, where ρ is the spectral radius, is given by

$$R_0 = \frac{\beta_1\kappa\sigma}{(\mu+\sigma)(\gamma_2+\tau_2+\mu)} + \frac{\rho\beta_1(1-\kappa)\sigma}{(\mu+\sigma)(\gamma_1+\tau_1+\mu)}$$

Using Theorem 2 in [29], the following result is established.

Lemma 4.3. *The DFE, ε_0, of the model (2.1) is locally-asymptotically stable (LAS) if $R_0 < 1$, and unstable if $R_0 > 1$.*

The threshold quantity, R_0 is the basic reproduction number of the disease [13; 8; 7]. This represent the average number of secondary cases generated by a infected person in a fully susceptible population. The epidemiological significance of 4.3 is that when R_0 is less than unity, a low influx of infected individuals into the population will not cause major outbreaks, and the disease would die out in time.

4.3. Global stability of DFE

Theorem 4.1. *The DFE of the model (2.1) is globally asymptotically stable in Ω whenever $R_0 \leq 1$.*

Proof. Consider the following Lyapunov function

$$\mathcal{L} = \Big(\frac{\sigma(\kappa k_2 + \rho(1-\kappa)k_3)}{k_1 k_2}\Big)E + \Big(\frac{\rho k_3}{k_2}\Big)A + I$$

where $k_1 = \mu + \sigma$, $k_2 = \gamma_1 + \tau_1 + \mu$ and $k_3 = \gamma_2 + \tau_2 + \mu$.
We take the Lyapunov derivative with respect to t,

$$\begin{aligned}
\dot{\mathcal{L}} &= \Big(\frac{\sigma(\kappa k_2 + \rho(1-\kappa)k_3)}{k_1 k_2}\Big)\dot{E} + \Big(\frac{\rho k_3}{k_2}\Big)\dot{A} + \dot{I} \\
&= \frac{\sigma(\kappa k_2 + \rho(1-\kappa)k_3)}{k_1 k_2}\Big[\frac{\beta_1 S(I+\rho A)}{N} - k_1 E\Big] + \frac{\rho k_3}{k_2}[(1-\kappa)\sigma E - k_2 A] + (\kappa\sigma E - k_3 I) \\
&\leq \frac{\beta_1\sigma(\kappa k_2 + \rho(1-\kappa)k_3)}{k_1 k_2}(I+\rho A) - \frac{\sigma(\kappa k_2 + \rho(1-\kappa)k_3)}{k_2}E + \frac{\rho(1-\kappa)k_3\sigma}{k_2}E \\
&- \rho k_3 A + \kappa\sigma E - k_3 I \text{ (Since } S \leq N \text{ in } \Omega) \\
&= \frac{\beta_1\sigma(\kappa k_2 + \rho(1-\kappa)k_3)}{k_1 k_2}(I+\rho A) - \rho k_3 A - k_3 I \\
&= \frac{\beta_1\sigma(\kappa k_2 + \rho(1-\kappa)k_3)}{k_1 k_2 k_3}k_3(I+\rho A) - \rho k_3 A - k_3 I \\
&= k_3(R_0 - 1)(I + \rho A) \leq 0, \text{ whenever } R_0 \leq 1.
\end{aligned}$$

Since all the variables and parameters of the model (2.1) are non-negative, it follows that $\dot{\mathcal{L}} \leq 0$ for $R_0 \leq 1$ with $\dot{\mathcal{L}} = 0$ in diseases free equilibrium. Hence, $\mathcal{L}$ is a Lyapunov function on Ω. Therefore, followed by LaSalles Invariance Principle [15], that

$$(E(t), A(t), I(t)) \to (0, 0, 0) \text{ as } t \to \infty \tag{A-2}$$

Since $\lim_{t\to\infty} supA(t) = 0$ and $\lim_{t\to\infty} supI(t) = 0$ (from A-2), it follows that, for sufficiently small $\epsilon > 0$, there exist constants $B_1 > 0$ and $B_2 > 0$ such that $\lim_{t\to\infty} supA(t) \leq \epsilon$ for all $t > B_1$ and $\lim_{t\to\infty} supI(t) \leq \epsilon$ for all $t > B_2$.
Hence, it follows from the fifth equation of the model (2.1) that, for $t > max\{B_1, B_2\}$,

$$\frac{dC}{dt} \leq \tau_1\epsilon + \tau_2\epsilon - k_4 C$$

Therefore using comparison theorem [26]

$$C^{\infty} = \lim_{t\to\infty} supC(t) \leq \frac{\tau_1\epsilon + \tau_2\epsilon}{k_4}$$

So as $\epsilon \to 0$, $C^{\infty} = \lim_{t\to\infty} supC(t) \leq 0$
Similarly (by using $\lim_{t\to\infty} infA(t) = 0$ and $\lim_{t\to\infty} infI(t) = 0$, it can be shown that

$$C_{\infty} = \lim_{t\to\infty} infC(t) \geq 0$$

Thus, it follows from above two relations

$$C_\infty \geq 0 \geq C^\infty$$

Hence $\lim_{t\to\infty} C(t) = 0$
Similarly, it can be shown that

$$\lim_{t\to\infty} R(t) = 0, \lim_{t\to\infty} S(t) = \frac{\Pi_H}{\mu}$$

Therefore by combining all above equations, it follows that each solution of the model equations (2.1), with initial conditions $\in \Omega$, approaches ε_0 as $t \to \infty$ for $R_0 \leq 1$. □

4.4. Existence and stability of endemic equilibria

In this section, the existence of the endemic equilibrium of the model (2.1) is established. Let us denote

$$k_1 = \mu + \sigma, k_2 = \gamma_1 + \tau_1 + \mu, k_3 = \gamma_2 + \tau_2 + \mu, k_4 = \delta + \gamma_3 + \mu.$$

Let $\varepsilon^* = (S^*, E^*, A^*, I^*, C^*, R^*)$ represents any arbitrary endemic equilibrium point (EEP) of the model (2.1). Further, define

$$\lambda^* = \frac{\beta_1(I^* + \rho A^*)}{N^*} \tag{A-3}$$

It follows, by solving the equations in (2.1) at steady-state, that

$$\begin{aligned} S^* &= \frac{\Pi_H}{\lambda^* + \mu}, E^* = \frac{\lambda^* S^*}{k_1}, A^* = \frac{(1-\kappa)\sigma\lambda^* S^*}{k_1 k_2}, \\ I^* &= \frac{\kappa\sigma\lambda^* S^*}{k_1 k_3}, C^* = \frac{(\tau_1(1-\kappa)\sigma\lambda^* k_3 + \tau_2\kappa\sigma\lambda^* k_2)S^*}{k_1 k_2 k_3 k_4} \\ R^* &= \frac{[\gamma_1(1-\kappa)\sigma\lambda^* k_3 k_4 + \gamma_2\kappa\sigma\lambda^* k_2 k_4 + \gamma_3\tau_1(1-\kappa)\sigma\lambda^* k_3 + \gamma_3\tau_2\kappa\sigma\lambda^* k_2]S^*}{\mu k_1 k_2 k_3 k_4} \end{aligned} \tag{A-4}$$

Substituting the expression in (A-4) into (A-3) shows that the non-zero equilibrium of the model (2.1) satisfy the following linear equation, in terms of λ^*:

$$a_0\lambda^* + a_1 = 0 \tag{A-5}$$

where

$$\begin{aligned} a_0 &= \mu[k_2 k_3 k_4 + (1-\kappa)\sigma\mu k_3 k_4 + \kappa\sigma\mu k_2 k_4 + \mu\tau_1(1-\kappa)\sigma k_3 + \mu\gamma_3 + \kappa\sigma k_2 k_4 \\ &\quad + \gamma_1(1-\kappa)\sigma k_3 k_4 + \gamma_2\kappa\sigma k_2 k_4 + \gamma_3\tau_1(1-\kappa)\sigma k_3 + \gamma_3\tau_2\kappa\sigma k_2 \\ a_1 &= \mu k_1 k_2 k_3 k_4(1 - R_0) \end{aligned}$$

Since $a_0 > 0$, $\mu > 0$, $k_1 > 0$, $k_2 > 0$, $k_3 > 0$ and $k_4 > 0$, it is clear that the model (2.1) has a unique endemic equilibrium point (EEP) whenever $R_0 > 1$ and no positive endemic equilibrium point whenever $R_0 < 1$. This rules out the possibility of the existence of equilibrium other than DFE whenever $R_0 < 1$. Furthermore, it can be shown that, the DFE ε_0 of the model (2.1) is globally asymptotically stable (GAS) whenever $R_0 < 1$.

From the above discussion we have concluded that

Theorem 4.2. *The model (2.1) has a unique endemic (positive) equilibrium, given by ε^*, whenever $R_0 > 1$ and has no endemic equilibrium for $R_0 \leq 1$.*

Now we will prove the local stability of endemic equilibrium.

Theorem 4.3. *The endemic equilibrium ε^* is locally asymptotically stable if $R_0 > 1$.*

Proof. The Jacobian matrix of the system (2.1) J_{ε_0} at DFE is given by

$$J_{\varepsilon_0} = \begin{bmatrix} -\mu & 0 & -\rho\beta_1 & -\beta_1 & 0 & 0 \\ 0 & -(\mu+\sigma) & \rho\beta_1 & \beta_1 & 0 & 0 \\ 0 & (1-\kappa)\sigma & -(\gamma_1+\tau_1+\mu) & 0 & 0 & 0 \\ 0 & \kappa\sigma & 0 & -(\gamma_2+\tau_2+\mu) & 0 & 0 \\ 0 & 0 & \tau_1 & \tau_2 & -(\delta+\gamma_3+\mu) & 0 \\ 0 & 0 & \gamma_1 & \gamma_2 & \gamma_3 & -\mu \end{bmatrix},$$

Here, by taking β_1 as a bifurcation parameter, we use the central manifold theory method to determine the local stability of the endemic equilibrium [9]. Taking β_1 as the bifurcation parameter and gives critical value of β_1 at $R_0 = 1$ is given as

$$\beta_1^* = \frac{(\mu+\sigma)(\gamma_1+\tau_1+\mu)(\gamma_2+\tau_2+\mu)}{[\kappa\sigma(\gamma_1+\tau_1+\mu)+(1-\kappa)\rho\sigma(\gamma_2+\tau_2+\mu)]}$$

The Jacobian of (2.1) at $\beta_1 = \beta_1^*$, denoted by $J_{\varepsilon_0}|_{\beta_1=\beta_1^*}$ has a right eigenvector (corresponding to the zero eigenvalue) given by $w = (w_1, w_2, w_3, w_4, w_5, w_6)^T$, where

$$\begin{aligned} w_1 &= -\frac{\mu+\sigma}{\mu}w_2, w_2 = w_2 > 0, w_3 = \frac{(1-\kappa)\sigma}{\gamma_1+\tau_1+\mu}w_2, w_4 = \frac{\kappa\sigma}{\gamma_2+\tau_2+\mu}w_2, \\ w_5 &= \frac{\tau_1(1-\kappa)\sigma(\gamma_2+\tau_2+\mu)+\tau_2\kappa\sigma(\gamma_1+\tau_1+\mu)}{(\gamma_1+\tau_1+\mu)(\gamma_2+\tau_2+\mu)(\delta+\gamma_3+\mu)}w_2, \\ w_6 &= \frac{\gamma_1(1-\kappa)\sigma}{\mu(\gamma_1+\tau_1+\mu)} + \frac{\gamma_2\kappa\sigma}{\mu(\gamma_2+\tau_2+\mu)} + \frac{\gamma_3\tau_1(1-\kappa)\sigma}{\mu(\gamma_1+\tau_1+\mu)(\delta+\sigma_3+\mu)} \\ &\quad + \frac{\gamma_3\tau_2\kappa\sigma}{\mu(\gamma_2+\tau_2+\mu)(\delta+\gamma_3+\mu)} \end{aligned}$$

Similarly, from $J_{\varepsilon_0}|_{\beta_1=\beta_1^*}$, we obtain a left eigenvector $v = (v_1, v_2, v_3, v_4, v_5, v_6)$ (corresponding to the zero eigenvalue), where

$$v_1 = 0, v_2 = v_2 > 0, v_3 = \frac{\rho\beta_1^*}{\gamma_1+\tau_1+\mu}v_2, v_4 = \frac{\beta_1^*}{\gamma_2+\tau_2+\mu}v_2, v_5 = 0, v_6 = 0.$$

Selecting the notations $S = x_1$, $E = x_2$, $A = x_3$, $I = x_4$, $C = x_5$, $R = x_6$ and $\frac{dx_i}{dt} = f_i$. Now we calculate the following second-order partial derivatives of f_i at the disease-free equilibrium ε_0 and obtain

$$\frac{\partial f_2}{\partial x_3 \partial x_2} = -\frac{\rho\beta_1\mu}{\Pi_H}, \frac{\partial f_2}{\partial x_4 \partial x_2} = -\frac{\beta_1\mu}{\Pi_H}, \frac{\partial f_2}{\partial x_3 \partial x_3} = -\frac{\rho\beta_1\mu}{\Pi_H}, \frac{\partial f_2}{\partial x_4 \partial x_3} = -\frac{\beta_1\mu}{\Pi_H}, \frac{\partial f_2}{\partial x_3 \partial x_4} = -\frac{\rho\beta_1\mu}{\Pi_H},$$
$$\frac{\partial f_2}{\partial x_4 \partial x_4} = -\frac{\beta_1\mu}{\Pi_H}, \frac{\partial f_2}{\partial x_3 \partial x_5} = -\frac{\rho\beta_1\mu}{\Pi_H}, \frac{\partial f_2}{\partial x_4 \partial x_5} = -\frac{\beta_1\mu}{\Pi_H}, \frac{\partial f_2}{\partial x_3 \partial x_6} = -\frac{\rho\beta_1\mu}{\Pi_H}, \frac{\partial f_2}{\partial x_4 \partial x_6} = -\frac{\beta_1\mu}{\Pi_H}.$$

Now we calculate the coefficients a and b defined in Theorem 4.1 [9] of Castillo-Chavez and Song as follow

$$a = \sum_{k,i,j=1}^{6} v_k w_i w_j \frac{\partial^2 f_k(0,0)}{\partial x_i \partial x_j}$$

and

$$b = \sum_{k,i=1}^{6} v_k w_i \frac{\partial^2 f_k(0,0)}{\partial x_i \partial \beta}$$

Replacing the values of all the second-order derivatives measured at DFE and $\beta_1 = \beta_1^*$, we get

$$a = -\frac{\beta_1^* v_2 \mu}{\Pi_H}(\rho w_3 + w_4)(w_2 + w_3 + w_4 + w_5 + w_6) < 0$$

and

$$b = v_2(\rho w_3 + w_4) > 0$$

Since $a < 0$ and $b > 0$ at $\beta_1 = \beta_1^*$, therefore using the Remark 1 of the Theorem 4.1 stated in [9], a transcritical bifurcation occurs at $R_0 = 1$ and the unique endemic equilibrium is locally asymptotically stable for $R_0 > 1$. □

Appendix B: Tables

Table B1: **Estimated parameter values of the model (2.1). All data are given in the format [Mean(95% CI)].**

Location	β_1	ρ	σ	κ	γ_1	τ_1	γ_2	τ_2
Maharashtra	22.5155 (1.79−23.57)	0.0016 (0.0003−0.0019)	0.3928 (0.08−0.95)	0.0387 (0.036−0.29)	0.4778 (0.16−0.99)	0.4670 (0.03−0.68)	0.6116 (0.12−0.98)	0.00008 (0.000006−0.0001)
Delhi	3.1424 (2.82−25.28)	0.0017 (0.0001−0.009)	0.7095 (0.08−0.74)	0.9601 (0.16−0.99)	0.3810 (0.13−0.98)	0.0600 (0.0007−0.16)	0.6495 (0.06−0.98)	0.0027 (0.0002−0.026)
Tamil Nadu	4.7292 (4.51−14.07)	0.2783 (0.007−0.28)	0.2136 (0.10−0.30)	0.9699 (0.62−0.99)	0.6316 (0.37−0.98)	0.0213 (0.002−0.112)	0.5465 (0.22−0.97)	0.0008 (0.0003−0.013)
India	3.0992 (3.07−10.74)	0.3298 (0.005−0.34)	0.2173 (0.07−0.23)	0.1059 (0.002−0.18)	0.3991 (0.1042−0.97)	0.0683 (0.0005−0.11)	0.3999 (0.09−0.71)	0.6996 (0.006−0.82)

Table B2: **Estimated initial values of the model (2.1). All data are given in the format [Mean(95% CI)].**

Location	$S(0)$	$E(0)$	$A(0)$	$I(0)$
Maharashtra	105529845 (101003959−124846987)	28.9356 (8.8032−464.5298)	13.6275 (1.1260−95.6263)	0.1164 (0.0010−0.1185)
Delhi	15715420 (10220425−19779270)	0.0477 (0.0030−0.2571)	13.6055 (4.1426−460.4245)	0.1516 (0.0076−2.6721)
Tamil Nadu	73422430 (73422426−73422451)	21.1188 (4.9809−96.0010)	94.7699 (85.5376−99.7557)	7.1954 (0.6844−22.1552)
India	1287838649 (1200296417−1293998633)	0.0019 (0.00001−0.0043)	0.2334 (0.0018−1.0616)	50.6837 (9.3315−148.6168)

Table B3: **Model prediction of notified cases in Maharashtra, Delhi, Tamil Nadu and India. All data are given in the format [Mean(95% CI)].**

Location	Total notified cases (no lock-down)	Total notified cases with lock-down success:20%	Total notified cases with lock-down success:40%	Total notified cases with lock-down success:60%	Total notified cases with lock-down success:80%	Prediction period
Maharashtra	12659 (541−5539012)	12651 (541−4682656)	12645 (541−4428012)	12641 (541−4293731)	12636 (541−4195833)	9/3/2020− 7/5/2020
Delhi	145323 (14034−506691)	101479 (13320−506690)	101422 (13156−506690)	98838 (13099−506690)	96829 (13068−506689)	17/3/2020− 15/5/2020
Tamil Nadu	175676 (68525−1068549)	138120 (54571−1068479)	131039 (52208−1068438)	127503 (51444−1068411)	125278 (51048−1068391)	18/3/2020− 16/5/2020
India	562366 (18601−74823924)	560737 (18591−50791004)	559840 (18584−45358767)	559193 (18578−42940818)	558637 (18572−41352158)	02/3/2020− 7/5/2020

Table B4: **Model prediction of notified deaths in Maharashtra, Delhi, Tamil Nadu and India. All data are given in the format [Mean(95% CI)].**

Location	Total notified deaths (no lock-down)	Total notified deaths with lock-down success-20%	Total notified deaths with lock-down success-40%	Total notified deaths with lock-down success-60%	Total notified deaths with lock-down success-80%	Prediction period
Maharashtra	2026 (109−684511)	2018 (102−598225)	2017 (102−567542)	2016 (102−549984)	2015 (102−536732)	9/03/2020− 7/05/2020
Delhi	31321 (529−136573)	19169 (506−136566)	16858 (501−136566)	15690 (500−136566)	14949 (499−136566)	17/3/2020− 15/5/2020
Tamil Nadu	15308 (1636−114959)	10377 (1335−114946)	8981 (1281−114942)	8304 (1262−114939)	7890 (1252−114937)	18/3/2020− 16/5/2020
India	65492 (2675−9904896)	65339 (2667−6950777)	65248 (2666−6127334)	65177 (2665−5726199)	65116 (2664−5453678)	02/3/2020− 7/5/2020

Table B5: **Estimated values of the basic reproduction number (R_0) for Maharashtra, Delhi, Tamil Nadu and overall India. All data are given in the format [Mean(95% CI)].**

Location	**Basic Reproduction Number (R_0)**
Maharashtra	1.46 (1.26−2.30)
Delhi	4.62 (3.70−5.40)
Tamil Nadu	8.44 (5.20−13.23)
India	2.25 (1.97−4.72)